

Straight and twisted Weyl nodal line phonons in Ho_2CF_2 material

Xin-Yue Kang(康鑫越), Jin-Yang Li(李金洋), and Si Li(李思)
Citation: Chin. Phys. B, 2023, 32 (**11**): 116301. DOI: 10.1088/1674-1056/aceaea
Journal homepage: http://cpb.iphy.ac.cn; http://iopscience.iop.org/cpb

What follows is a list of articles you may be interested in

Unveiling phonon frequency-dependent mechanism of heat transport across stacking fault in silicon carbide

Fu Wang(王甫), Yandong Sun(孙彦东), Yu Zou(邹宇), Ben Xu(徐贲), and Baoqin Fu(付宝勤)
Chin. Phys. B, 2023, 32 (**9**): 096301. DOI: 10.1088/1674-1056/acdfc0

Ab-initio calculations of bandgap tuning of $In_{1-x}Ga_xY$ (Y = N, P) alloys for optoelectronic applications

Muhammad Rashid, Jamil M, Mahmood Q, Shahid M Ramay, Asif Mahmood A, and Ghaithan H M
Chin. Phys. B, 2021, 30 (**11**): 116301. DOI: 10.1088/1674-1056/abf128

Inverted V-shaped evolution of superconducting temperature in SrBC under pressure

Ru-Yi Zhao(赵如意), Xun-Wang Yan(闫循旺), and Miao Gao(高淼)
Chin. Phys. B, 2021, 30 (**7**): 076301. DOI: 10.1088/1674-1056/abfbcc

Theoretical analysis of cross-plane lattice thermal conduction in graphite

Yun-Feng Gu(顾云风)
Chin. Phys. B, 2019, 28 (**6**): 066301. DOI: 10.1088/1674-1056/28/6/066301

Unconventional lattice dynamics in few-layer h-BN and indium iodide crystals

Gan Hu(胡干), Jian-Qi Huang(黄建啟), Ya-Ning Wang(王雅宁), Teng Yang(杨腾), Bao-Juan Dong(董宝娟), Ji-Zhang Wang(王吉章), Bo Zhao(赵波), Sajjad Ali(阿里·萨贾德), Zhi-Dong Zhang(张志东)
Chin. Phys. B, 2018, 27 (**8**): 086301. DOI: 10.1088/1674-1056/27/8/086301

SPECIAL TOPIC — Celebrating the 100th Anniversary of Physics Discipline of Northwest University

Straight and twisted Weyl nodal line phonons in Ho_2CF_2 material

Xin-Yue Kang(康鑫越)[1,2], Jin-Yang Li(李金洋)[1,2], and Si Li(李思)[1,2,†]

[1] *School of Physics, Northwest University, Xi'an* 710127, *China*
[2] *Shaanxi Key Laboratory for Theoretical Physics Frontiers, Xi'an* 710127, *China*

(Received 12 June 2023; revised manuscript received 17 July 2023; accepted manuscript online 27 July 2023)

Based on first-principles calculations, symmetry analysis and model construction, we predict that Ho_2CF_2 hosts both straight and twisted Weyl nodal lines in its bulk phonon spectrum. We identify that the top two phonon bands entangle with each other, forming two straight Weyl nodal lines on the K–H and K'–H' paths at the Brillouin zone (BZ) boundary, and six twisted Weyl nodal lines within the BZ. All the Weyl nodal lines along the k_z direction and across the entire BZ. The symmetry analysis indicates that these Weyl nodal lines are protected by the $\mathcal{PT}$ symmetry and crystal symmetry. The Berry phase and drumhead-like nontrivial surface states are calculated. We also construct a tight-binding model to describe these nodal lines. Our work provides an excellent material platform for exploring the fascinating physics associated with straight and twisted Weyl nodal line phonons.

Keywords: topological quasiparticles, topological phonons, straight nodal lines, twisted nodal lines

PACS: 63.20.D–, 03.65.Vf, 03.75.Lm, 73.20.–r **DOI:** 10.1088/1674-1056/aceaea

1. Introduction

In the past decade, there has been a significant surge of research interest in the topological quasiparticles that emerge around band degeneracy points in condensed matter systems.[1–3] Based on the dimension of the band degeneracy within the Brillouin zone (BZ) in momentum space, topological quasiparticles can be categorized as zero-dimensional (0D) node points (such as Weyl and Dirac semimetals),[4–8] one-dimensional (1D) nodal lines[9–19] and two-dimensional (2D) nodal surfaces.[20–23] Due to these degeneracies in topological quasiparticles, the low-energy electron excitations are endowed with various exotic physical properties.

Topological quasiparticles were studied in electronic band structures at first and then the study was extended to bosonic and even classical systems, such as photonic crystals,[24–26] acoustic systems,[27–29] and electric circuit networks.[30–32] Phonons are the fundamental bosonic excitations in a crystal material, describing the collective motion of an atomic lattice. Unlike electronic fermions, phonons are not constrained by the Pauli exclusion principle. Consequently, the entire frequency range of a phonon spectrum can be experimentally explored. Recently, topological quasiparticles in phonons have been attracting a great deal of attention.[33–42]

As an interesting type of topological quasiparticles, topological nodal line semimetals, which are band degeneracy curves between the conduction and valence bands in a BZ, have been attracting significant interest due to their variety of intriguing properties, such as drumhead-like surface states,[10] anisotropic electron transport,[12] an unusual optical response and circular dichroism,[43–45] possible surface magnetism and superconductivity,[16,46–48] and density fluctuation plasmons and Friedel oscillations.[49] In addition, topological nodal lines can be classified into various types based on their geometry, such as nodal rings,[13–15] nodal chains,[50,51] nodal links,[52–54] and even nodal knots.[55,56] These topological nodal lines all have closed configurations. Recently, straight nodal lines and twisted nodal lines that extend in a certain direction and traverse the entire bulk BZ have been discovered, and several concrete materials hosting such nodal lines have been proposed.[18,38,57–60] However, the number of candidates is still very limited. Hence, there is a need to explore more realistic materials that can realize straight and twisted Weyl nodal lines.

In this work, through first-principles calculations and symmetry analysis, we report that Ho_2CF_2 material hosts both straight Weyl nodal lines and twisted Weyl nodal lines in its bulk phonon spectrum. We find that the crossing points between the top two phonon bands form two straight Weyl nodal lines at the BZ boundary and six twisted Weyl nodal lines within the BZ. Here, all the straight and twisted Weyl nodal lines extend along the k_z direction and across the entire BZ and they are topologically distinct from those which do not penetrate the BZ. The results of symmetry analysis and the nontrivial π Berry phase are demonstrated. The corresponding nontrivial surface states are revealed. We also construct a tight-binding (TB) model to capture these nodal lines. Our findings suggest an exceptionally suitable platform for experimentally exploring the intriguing properties of straight and twisted Weyl nodal line phonons.

[†]Corresponding author. E-mail: sili@nwu.edu.cn

© 2023 Chinese Physical Society and IOP Publishing Ltd

2. Crystal structure

Ho_2CF_2 belongs to the rare earth carbide fluoride compounds and it has been successfully synthesized in experiments.[61] The crystal structure has been determined by a quantitative analysis of the x-ray diffraction data (the crystal structure data are $a = b = 3.6567$ Å and $c = 6.3171$ Å).[61] Ho_2CF_2 crystalizes into a trigonal structure with space group No. 164 ($P\bar{3}m1$), which can be generated by the following symmetry elements: S_6^+ and C_2''. The crystal structures of Ho_2CF_2 and the BZ are schematically shown in Fig. 1. The Wyckoff positions of the Ho, C and F atoms are 2*d* (1/3, 2/3, 0.2098), 1*a* (0, 0, 0) and 2*d* (1/3, 2/3, 0.6175), respectively.

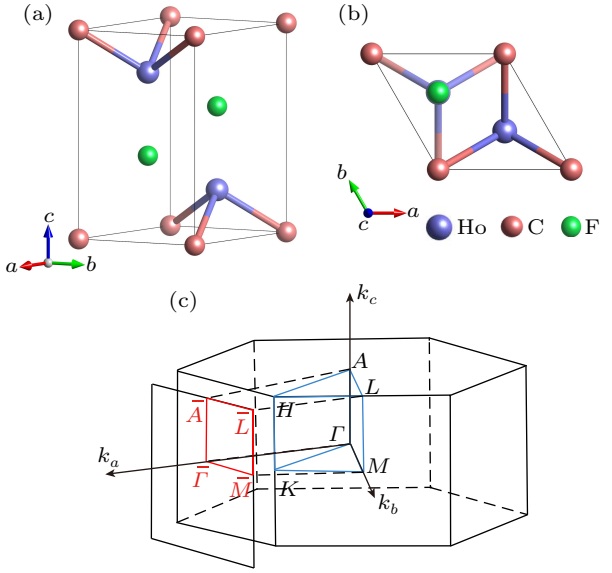


Fig. 1. (a) Side view and (b) top view of the crystal structure of Ho_2CF_2. The primitive cell is shown with a solid line. (c) Bulk BZ and the projected surface BZ of the (100) plane. The high-symmetry points are labeled.

3. First-principles methods

The density functional theory (DFT) was employed for first-principles calculations, utilizing the projector-augmented wave method as implemented in the Vienna *ab initio* simulation package.[62–64] The exchange–correlation functional employed the Perdew–Burke–Ernzerhof[65] realization within the generalized gradient approximation. The plane wave energy cutoff was set to 600 eV and the BZ was sampled using a Γ-centered k mesh of size $15 \times 15 \times 8$. The convergence criteria for energy and force were set to 10^{-7} eV and 10^{-3} eV/Å, respectively. The structure is fully optimized. The optimized lattice parameters for the Ho_2CF_2 are $a = b = 3.638$ Å and $c = 6.416$ Å, which are close to the experimental values ($a = b = 3.6567$ Å and $c = 6.3171$ Å). The force constants and phonon spectra were obtained using the density functional perturbation theory in combination with the Phonopy package.[66] The irreducible representations of the phonon spectra were calculated using the PhononIrep package.[67] The surface states were calculated using the Green's function method based on the WannierTools package.[68–70]

4. Results

4.1. Straight and twisted Weyl nodal line phonons

The phonon spectrum of Ho_2CF_2 obtained from first-principles calculations is shown in Fig. 2(a). From Fig. 2(a), one can observe that three phonon bands (the 13th to the 15th bands) between 10.8 THz and 18 THz separate from other phonon bands and entangle together. Among the three phonon bands, the crossing between the top two phonon bands (14th and 15th) forms a twofold degenerate along the K–H path and linear band-crossing points along the Γ–K and H–A paths. Via a careful scan of the BZ, we find that these degenerate points form two straight Weyl nodal lines along paths K–H and K'–H' at the BZ boundary and six twisted Weyl nodal lines within the BZ, as shown in Figs. 2(b) and 2(c), respectively. Particularly, the phonon band structure around the straight and twisted Weyl nodal lines is very "clean", since the crossing points of the nodal lines are located in the gap between the 14th and 15th phonon bands and there are no other extraneous bands nearby. Meanwhile, the nodal lines are exposed in a large frequency window with a width of about 1 THz. The frequency of the nodal lines can be inferred from the dip in the phonon density of states. The clean phonon band structure, the large frequency window and the small frequency variation on the nodal lines make Ho_2CF_2 an almost ideal candidate for experimental studies of straight and twisted Weyl nodal line phonons.

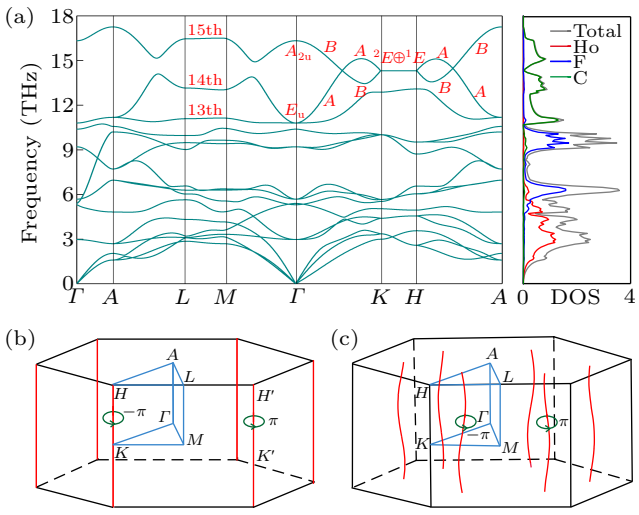


Fig. 2. (a) Calculated phonon spectrum and phonon density of states for Ho_2CF_2. The irreducible representations (IRRs) are given. Distribution of straight Weyl nodal lines (b) and twisted Weyl nodal lines (c) in the BZ for Ho_2CF_2 obtained from the DFT calculation.

Here, both the straight and twisted Weyl nodal lines traverse the whole BZ in the k_z direction. This type of nodal line is topologically different from those that do not traverse the BZ because the former cannot be continuously contracted to a

point, while the latter can. Mathematically, the BZ is topologically equivalent to a three-dimensional torus denoted as $\mathbb{T}^3$. Closed loops on $\mathbb{T}^3$ can be categorized based on their fundamental homotopy group $\pi_1(\mathbb{T}^3) = Z^3$, which is described by three integers representing the number of times the loop winds around each of the three directions.[18] From this perspective, the nodal lines that do not traverse the BZ belong to the trivial class with $Z^3 = (0,0,0)$, while the nodal lines discussed here belong to the class $(0,0,1)$.

Since the straight and twisted Weyl nodal lines extend along the k_z direction and display strong anisotropy in the dispersion relation, they may result in pronounced anisotropic transport.

4.2. Symmetry protection and Berry phase

The straight Weyl nodal lines along paths K–H and K'–H' are protected by two independent symmetries: $\mathcal{PT}$ symmetry and C_{3z} symmetry. Phonons are intrinsically spinless and the presence of $\mathcal{PT}$ symmetry requires that the Berry phase associated with any closed path must be quantized into multiples of π.[71] In this context, the Berry phase is given by the equation

$$\gamma_\ell = \sum_{n\in \text{occ.}} \oint_\ell \langle u_n(\boldsymbol{k}) | \mathrm{i}\nabla_{\boldsymbol{k}} u_n(\boldsymbol{k})\rangle \mathrm{d}\boldsymbol{k}. \tag{1}$$

Here, the Berry phase is computed for a locally gapped spectrum along a closed path ℓ. The term $|u_n(\boldsymbol{k})\rangle$ represents the periodic part of the Bloch eigenstate. For a nodal line, we can calculate its Berry phase γ_ℓ for a closed path ℓ encircling the nodal line. Through DFT calculations, we find that the Berry phases for the straight Weyl nodal lines along paths K–H and K'–H' are $-\pi$ and π [see Fig. 2(b)], respectively, showing that the straight nodal lines are topologically nontrivial.

Another protection for the straight Weyl nodal lines is from the C_{3z} symmetry. The straight nodal lines lie on the K–H and K'–H' high-symmetry lines, which are invariant under C_{3z}. Thus, each state on these high-symmetry lines is also an eigenstate of C_{3z}, with an eigenvalue $g_{3z} = \mathrm{e}^{\pm \mathrm{i}2\pi/3}$. The nodal line is protected if the two degenerate bands have different g_{3z} on the K–H (K'–H') path. In fact, the IRRs of the two phonon bands calculated by our DFT is ${}^2E \oplus {}^1E$ [see Fig. 2(a)], which can allow the existence of twofold degeneracy. The IRRs ${}^2E \oplus {}^1E$ of C_{3z} correspond to $\begin{bmatrix} \mathrm{e}^{\mathrm{i}2\pi/3} & 0 \\ 0 & \mathrm{e}^{-\mathrm{i}2\pi/3} \end{bmatrix}$, which indicates that the twofold degenerate bands at K–H path have a different C_{3z} eigenvalues $\mathrm{e}^{\mathrm{i}2\pi/3}$ and $\mathrm{e}^{-\mathrm{i}2\pi/3}$. In addition, the C_{3z} symmetry further pins the straight nodal line to be on the K–H (K'–H') high-symmetry line.

Similarly, the twisted Weyl nodal lines are protected by the $\mathcal{PT}$ symmetry and C_2'' symmetry. The $\mathcal{PT}$ symmetry requires that the Berry phase for any closed path encircling the twisted Weyl nodal line is $\pm\pi$, which is also confirmed by our DFT calculations, as shown in Fig. 2(c). The two crossing phonon bands near the nodal point on the twisted Weyl nodal line have different IRRs A and B [along the path Γ–K and H–A, as shown in Fig. 2(a)], which correspond to the opposite C_2'' eigenvalue 1 and -1.

4.3. Drumhead-like surface states

One of the important signatures of the topological nodal line is the presence of drumhead-like surface states at the sample surface.[10] In Fig. 3, we plot the calculated surface phonon spectrum for the (100) surface of Ho_2CF_2. One indeed observes a surface band connecting the nodal points that correspond to the nodal line in the bulk, as indicated by the green arrows in Fig. 3. The surface band connects the nodal lines through the surface BZ boundary. We also plot the isofrequency surface contour at 14.5 THz of the (100) surface in Fig. 3(b).

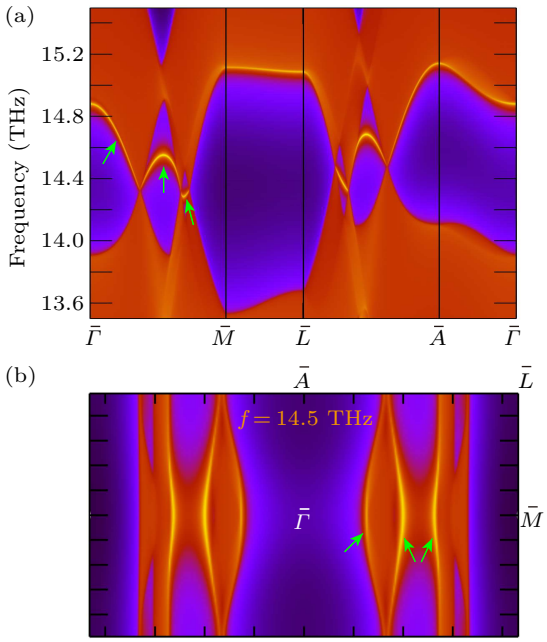


Fig. 3. (a) Calculated surface phonon spectrum for the (100) surface and (b) the corresponding isofrequency surface contour at 14.5 THz. The green arrows indicate the drumhead-like surface states.

4.4. TB model

To further characterize the straight and twisted Weyl nodal lines, we construct a TB model based on the symmetry requirements. We consider one atom occupying the Wyckoff position 1a (0, 0, 0) within a unit cell with three p-like basis orbitals (p_x, p_y, and p_z) in each site. We consider the nearest-neighbor hopping, the spinless TB model is constructed using the MagneticTB package[72] and the model is given by

$$H = \begin{bmatrix} e_1+\eta_1 & \eta_2 & \eta_3 \\ \eta_2^* & e_1+\eta_4 & \eta_5 \\ \eta_3^* & \eta_5^* & e_2+\eta_6 \end{bmatrix}, \tag{2}$$

where η_i is given by

$$\eta_1 = \frac{2}{\sqrt{3}} t_1 [\cos(k_x) - 2\cos(k_y) - 2\cos(k_x + k_y)]$$

$$
\begin{aligned}
&+2t_2[\cos(k_x)+\cos(k_y)+\cos(k_x+k_y)],\\
\eta_2 &= -2t_1[\cos(k_y)-\cos(k_x+k_y)],\\
\eta_3 &= 2\sqrt{3}t_3[\cos(k_y)-\cos(k_x+k_y)],\\
\eta_4 &= -2\sqrt{3}t_1\cos(k_x)\\
&\quad +2t_2[\cos(k_x)+\cos(k_y)+\cos(k_x+k_y)],\\
\eta_5 &= -2t_3[2\cos(k_x)-\cos(k_y)-\cos(k_x+k_y)],\\
\eta_6 &= 2t_4[\cos(k_x)+\cos(k_y)+\cos(k_x+k_y)],
\end{aligned}
\tag{3}
$$

where e_i, t_i are real model parameters and the wave vectors are measured in units of the respective inverse lattice constant. The phonon bands calculated by the TB model are shown in Fig. 4, which shows that our TB model accurately captures the dispersion features of the straight and twisted Weyl nodal line phonons in Ho_2CF_2.

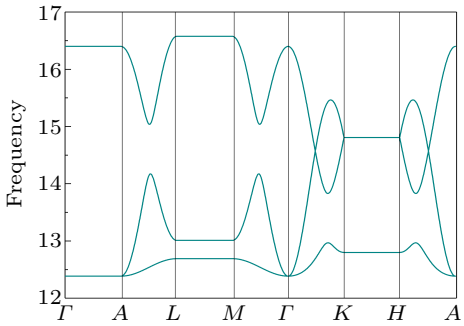


Fig. 4. The calculated phonon bands using the tight-binding (2) model. In the calculation, we set $e_1 = e_2 = 14$, $t_1 = -0.4$, $t_2 = -0.5$, $t_3 = 0.1$, $t_4 = 0.4$.

5. Conclusion

In conclusion, we have theoretically predicted the existence of both straight and twisted Weyl nodal line phonons in Ho_2CF_2. These nodal lines traverse the whole BZ along the k_z direction. The results of the symmetry analysis and Berry phase calculations indicated that these nodal lines have symmetry protection and are topologically nontrivial. In addition, drumhead-like surface states occur on the (100) surface. We have constructed a TB model to describe these nodal lines. In an experiment, the bulk straight and twisted Weyl nodal line phonons can be directly probed in neutron scattering[73] and x-ray scattering[74] (for example, the helical nodal lines in the phonon spectrum of MoB_2 have been probed by inelastic x-ray scattering[38]), and the surface states could be probed by high-resolution electron energy loss spectroscopy,[75] helium scattering,[76] and THz spectroscopy.[77,78] Our results offer a promising platform for exploring the intriguing physics associated with straight and twisted Weyl nodal line phonons.

Acknowledgment

Project supported by the National Natural Science Foundation of China (Grant No. 12204378).

References

[1] Elliott S R and Franz M 2015 *Rev. Mod. Phys.* **87** 137
[2] Armitage N P, Mele E J and Vishwanath A 2018 *Rev. Mod. Phys.* **90** 015001
[3] Yu Z M, Zhang Z Y, Liu G B, Wu W K, Li X P, Zhang R W, A Yang S Y and Yao Y G 2022 *Sci. Bull.* **67** 375
[4] Murakami S 2007 *New J. Phys.* **9** 356
[5] Wan X G, Turner A M, Vishwanath A and Savrasov S Y 2011 *Phys. Rev. B* **83** 205101
[6] Young S M, Zaheer S, Teo J C Y, Kane C L, Mele E J and Rappe A M 2012 *Phys. Rev. Lett.* **108** 140405
[7] Wang Z J, Sun Y, Chen X Q, Franchini C, Xu G, Weng H M, Dai X and Fang Z 2012 *Phys. Rev. B* **85** 195320
[8] Wang Z J, Weng H M, Wu Q S, Dai X and Fang Z 2013 *Phys. Rev. B* **88** 125427
[9] Burkov A, Hook M D and Balents L 2011 *Phys. Rev. B* **84** 235126
[10] Weng H M, Liang Y Y, Xu Q, Yu R, Fang Z, Dai X and Kawazoe Y 2015 *Phys. Rev. B* **92** 045108
[11] Chen Y P, Xie Y, Yang S A, Pan H, Zhang F, Cohen M L and Zhang S B 2015 *Nano Lett.* **15** 6974
[12] Mullen K, Uchoa B and Glatzhofer D T 2015 *Phys. Rev. Lett.* **115** 026403
[13] Yu R, Weng H M, Fang Z, Dai X and Hu X 2015 *Phys. Rev. Lett.* **115** 036807
[14] Kim Y, Wieder B J, Kane C L and Rappe A M 2015 *Phys. Rev. Lett.* **115** 036806
[15] Fang C, Chen Y G, Kee H Y and Fu L 2015 *Phys. Rev. B* **92** 081201
[16] Li R H, Ma H, Cheng X Y, Wang S L, Li D Z, Zhang Zheng Y, Li Y Y and Chen X Q 2016 *Phys. Rev. Lett.* **117** 096401
[17] Bian G, Chang T R, Sankar R, Xu S Y, Zheng H, Neupert T, Chiu C K, Huan S M, Chang G Q, Belopolski I, *et al.* 2016 *Nat. Commun.* **7** 10556
[18] Li S, Yu Z M, Liu Y, Guan S, Wang S S, Zhang X M, Yao Y G and Yang S A 2017 *Phys. Rev. B* **96** 081106
[19] Li S, Liu Y, Wang, Wang S S, Yu, Yu Z M, Guan S, Sheng X L, Yao Y G and Yang S A 2018 *Phys. Rev. B* **97** 045131
[20] Zhong C Y, Chen Y P, Xie Y, Yang S A, Cohen M L and Zhang S B 2016 *Nanoscale* **8** 7232
[21] Liang Q F, Zhou J, Yu R, Wang Z and Weng H M 2016 *Phys. Rev. B* **93** 085427
[22] Bzdušek Táš and Sigrist M 2017 *Phys. Rev. B* **96** 155105
[23] Wu W K, Liu Y, Li S, Zhong C Y, Yu Z M, Sheng X L, Zhao Y X and Yang S A 2018 *Phys. Rev. B* **97** 115125
[24] Yang B, Guo Q H, Tremain B, Barr L E, Gao W L, Liu H C, Béri B, Xiang Y J, Fan D Y, Hibbins A P and others 2017 *Nat. Commun.* **8** 97
[25] Xie B Y, Wang H F, Zhu X Y, Lu M H, Wang Z D and Chen Y F 2018 *Opt. Express* **26** 24531
[26] Kim M, Jacob Z and Rho J 2020 *Light* **9** 130
[27] Li F, Huang X Q, Lu J Y, Ma J H and Liu Z Y 2018 *Nat. Phys.* **14** 30
[28] Ge H, Ni X, Tian Y, Gupta S K, Lu M H, Lin X, Huang W D, Chan C T and Chen Y F 2018 *Phys. Rev. Appl.* **10** 014017
[29] Xue H, Yang Y H and Zhang B 2022 *Nat. Rev. Mater.* **7** 974
[30] Luo K F, Yu R and Weng H M 2018 *Research*
[31] Lee C H, Imhof S, Berger C, Bayer F, Brehm J, Molenkamp L W, Kiessling T and Thomale R 2018 *Commun. Phys.* **1** 39
[32] Helbig T, Hofmann T, Lee C H, Thomale R, Imhof S, Molenkamp L W and Kiessling T 2019 *Phys. Rev. B* **99** 161114
[33] Zhang T T, Song Z D, Alexandradinata A, Weng H M, Fang C, Lu L and Fang Z 2018 *Phys. Rev. Lett.* **120** 016401
[34] Miao H, Zhang T T, Wang L, Meyers D, Said A H, Wang Y L, Shi Y G, Weng H M, Fang Z and Dean M 2018 *Phys. Rev. Lett.* **121** 035302
[35] Xia B W, Wang R, Chen Z J, Zhao Y J and Xu H 2019 *Phys. Rev. Lett.* **123** 065501
[36] Wang R, Xia B W, Chen Z J, Zheng B B, Zhao Y J and Xu H 2020 *Phys. Rev. Lett.* **124** 105303
[37] Chen Z J, Wang R, Xia B W, Zheng B B, Jin Y J, Zhao Y J and Xu H 2021 *Phys. Rev. Lett.* **126** 185301
[38] Zhang T T, Miao H, Wang Q, Lin J Q, Cao Y, Fabbris G, Said A H, Liu X, Lei H C, Fang Z, *et al.* 2019 *Phys. Rev. Lett.* **123** 245302
[39] Li J X, Liu J X, Baronett S A, Liu M F, Wang L, Li R H, Chen Y, Li D Z, Zhu Q and Chen X Q 2021 *Nat. Commun.* **12** 1204

[40] Xu Y F, Vergniory M G, Ma D S, Mañes J L, Song Z D, Bernevig B A, Regnault N and Elcoro L 2022 arXiv: 2211.11776

[41] Li S, Zhang Z Y, Feng X K, Wu W K, Yu Z M, Zhao Y X, Yao Y G and Yang S A 2023 *Phys. Rev. B* **107** 235145

[42] Kang X Y, Li J Y and Li S 2023 *Phys. Rev. B* **108** 125127

[43] Carbotte J P 2016 *J. Phys.: Condens. Matter.* **29** 045301

[44] Ahn S, Mele E J and Min H 2017 *Phys. Rev. Lett.* **119** 147402

[45] Liu Y, Yang S A and Zhang F 2018 *Phys. Rev. B* **97** 035153

[46] Chan Y H, Chiu C K, Chou M Y and Schnyder A P 2016 *Phys. Rev. B* **93** 205132

[47] Wang Y X and Nandkishore R M 2017 *Phys. Rev. B* **95** 060506

[48] Liu J P and Balents L 2017 *Phys. Rev. B* **95** 075426

[49] Rhim J W and Kim Y B 2016 *Phys. Rev. B* **18** 043010

[50] Bzdušek T, Wu Q S, Rüegg A, Sigrist M and Soluyanov A A 2016 *Nature* **538** 75

[51] Yan Q H, Liu R J, Yan Z B, Liu B Y, Chen H S, Wang Z and Lu L 2018 *Nat. Phys.* **14** 461

[52] Yan Z B, Bi R, Shen H T, Lu L, Zhang S C and Wang Z 2017 *Phys. Rev. B* **96** 041103

[53] Chen W, Lu H Z and Hou J M 2017 *Phys. Rev. B* **96** 041102

[54] Chang G Q, Xu S Y, Zhou X T, Huang S M, Singh B, Wang B K, Belopolski I, Yin J X, Zhang S T, Bansil A, *et al.* 2017 *Phys. Rev. Lett.* **119** 156401

[55] Bi R, Yan Z B, Lu L and Wang Z 2017 *Phys. Rev. B* **96** 201305

[56] Lee C H, Sutrisno A, Hofmann T, Helbig T, Liu Y H, Ang Y S, Ang L K, Zhang X, Greiter M and Thomale R 2020 *Nat. Commun.* **11** 4385

[57] Li J X, Xie Q, Liu J X, Li R H, Liu M, Wang L, Li D Z, Li Y Y and Chen X Q 2020 *Phys. Rev. B* **101** 024301

[58] Liu G, Jin Y J, Chen Z J and Xu H 2021 *Phys. Rev. B* **104** 024304

[59] Wang D Y, Yang B, Zhang R Y, Chen W J, Zhang Z Q, Zhang S and Chan C T 2022 *Phys. Rev. Lett.* **129** 043602

[60] Zhang T T, Yilmaz T, Vescovo E, Li H X, Moore R G, Lee H N, Miao H, Murakami S and McGuire M A 2022 *Npj Comput. Mater.* **8** 155

[61] Cockcroft J K, Kremer R K, Raju N P, Simon A, *et al.* 1992 *J. Alloys Compd.***183** 241

[62] Kresse G and Hafner J 1994 *Phys. Rev. B* **49** 14251

[63] Kresse G and Furthmüller J J 1996 *Phys. Rev. B* **54** 11169

[64] Blöchl P E 1994 *Phys. Rev. B* **50** 17953

[65] Perdew J P, Burke K and Ernzerhof M 1996 *Phys. Rev. Lett.* **77** 3865

[66] Togo A and Tanaka I 2015 *Scr. Mater.* **108** 1

[67] Zhang Z Y, Yu Z M, Liu G B and Yao Y G 2022 arXiv: 2201.11350

[68] Sancho M L, Sancho J L and Rubio J 1984*J. Phys. F: Met. Phys.***14** 1205

[69] Sancho M Lopez, Sancho J L, Sancho J L and Rubio J 1985 *J. Phys. F: Met. Phys.***15** 851

[70] Wu Q S, Zhang S N, Song H F, Troyer M and Soluyanov A A 2018 *Comput. Phys. Commun.***224** 405

[71] Zhao Y X, Schnyder A P and Wang Z D 2016 *Phys. Rev. Lett.* **116** 156402

[72] Zhang Z Y, Yu Z M, Liu G B and Yao Y G 2022 *Comput. Phys. Commun.* **270** 108153

[73] Delaire O, Al-Qasir I I, May A F, Li C W, Sales B C, Niedziela J L, Ma J, Matsuda M, Abernathy D L and Berlijn T 2015 *Phys. Rev. B* **91** 094307

[74] Mohr M, Maultzsch J, Dobardžić E, Reich S, Milošević I, Damnjanović M, Bosak A, Krisch M and Thomsen C 2007 *Phys. Rev. B* **76** 035439

[75] Zhu X T, Cao Y W, Zhang S Y, Jia X, Guo Q L, Yang F, Zhu L F, Zhang J D, Plummer E W and Guo J D 2015 *Rev. Sci. Instrum.* **86** 083902

[76] Harten U and Toennies J P 1987 *Europhys. Lett.* **4** 833

[77] Wu L, Salehi M, Koirala N, Moon J, Oh S and Armitage N P 2016 *Science* **354** 1124

[78] Wu L, Tse W K, Brahlek M, Morris C M, Aguilar R Valdés, Koirala N, Oh S and Armitage N P 2015 *Phys. Rev. Lett.* **115** 217602